

MERCURY-ARGON TWO-PHASE HEAT TRANSFER IN A VERTICAL ANNULUS UNDER TRANSVERSE MAGNETIC FIELD

I. MICHIOYOSHI, M. TANAKA and O. TAKAHASHI

Department of Nuclear Engineering, Kyoto University, Kyoto, Japan

(Received 5 August 1981)

Abstract—This paper presents experimental data of local properties and heat transfer of mercury-argon two-phase bubbly flow with small gas flow rate in a vertical annulus in the presence of transverse magnetic field. The two-phase Nusselt number decreases as well as single phase mercury heat transfer with increasing Hartmann number at the fixed Peclet number, but its decrease becomes smaller than the single phase as the quality is increased. Discussions are presented on contributions of effective thermal conductivity, eddy diffusivity of heat and liquid velocity to the two-phase heat transfer.

NOMENCLATURE

B ,	magnetic flux density [T];
D_i ,	outside diameter of inner wall, $D_i = 2R_i$ [mm];
D_o ,	inside diameter of outer wall, $D_o = 2R_o$ [mm];
d_e ,	equivalent diameter of annulus, $d_e = D_o - D_i$ [mm];
M ,	Hartmann number calculated for mercury, $M = \frac{1}{2}d_e B(\sigma_L/\mu_L)^{1/2}$;
N_{loc} ,	bubble number rate [count min ⁻¹];
Nu ,	Nusselt number, $Nu = qd_c/[(T_w - T_{bk})\lambda_L]$;
Pe ,	Peclet number calculated for mercury, $Pe = Pr \cdot Re$;
Pr ,	Prandtl number of mercury;
q ,	heat flux [W m ⁻²];
Re ,	Reynolds number calculated for mercury, $Re = 4W_L d_e/[\pi(D_o^2 - D_i^2)\mu_L]$;
r ,	radial coordinate [mm];
T ,	temperature [K];
u_m ,	superficial velocity of mercury, $u_m = 4W_L/[\pi\rho_L(D_o^2 - D_i^2)]$ [m s ⁻¹];
V ,	velocity [m s ⁻¹];
W ,	mass flow rate [kg s ⁻¹];
x ,	distance from upstream extremity of heating section [mm];
x_q ,	quality, $x_q = W_G/(W_G + W_L)$.

bk,	bulk of fluid;
G,	argon (gas);
L,	mercury (liquid);
TP,	two-phase flow;
w,	wall;
0,	no magnetic field is present, or single phase mercury flow.

INTRODUCTION

HEAT transfer characteristics of single phase flow of liquid metal in the presence of magnetic field have been studied theoretically and experimentally by many investigators. In this connection, Lielausis [1] has given a review on the liquid metal magnetohydrodynamics (MHD) and discussed the MHD problems in relation to nuclear power including the cooling blanket of a nuclear fusion reactor. The effect of magnetic field, however, on two-phase heat transfer has scarcely been analyzed.

On the other hand, when the magnetic field is not present, Mizushima *et al.* [2] have conducted the heat transfer experiments for mercury-nitrogen and mercury-helium two-phase flows in horizontal and vertical circular tubes, and also Ochiai *et al.* [3] for sodium-argon two-phase flow in a vertical tube, and they have shown the decrease of heat transfer coefficients. These results might be mainly due to the decrease of effective thermal conductivity because of the existence of gas bubbles near the heat transfer surface. This problem has been also theoretically treated by Hori *et al.* [4], Winterton [5] and Bishop *et al.* [6]. These papers, however, have not paid attention to the void fraction profile, bubble velocity, liquid velocity, and consequently the effect of agitation of bubbles, which are very important factors of two-phase heat transfer [7, 8].

This paper presents the experimental data of heat transfer of mercury-argon two-phase bubbly flow, of which gas flow rate is much smaller as compared with our previous report [9], in a vertical annulus in the presence of transverse magnetic field, together with the local properties of this two-phase flow.

Greek symbols

α ,	average void fraction [%];
α_{loc} ,	local void fraction [%];
ϵ_H ,	eddy diffusivity of heat [m ² s ⁻¹];
λ ,	thermal conductivity [W m ⁻¹ K ⁻¹];
μ ,	viscosity [kg m ⁻¹ s ⁻¹];
σ ,	electrical conductivity [mho m ⁻¹];
ρ ,	density [kg m ⁻³];
χ_{tt} ,	Lockhart-Martinelli modulus.

Subscripts

B ,	magnetic field is present;
b ,	bubble;

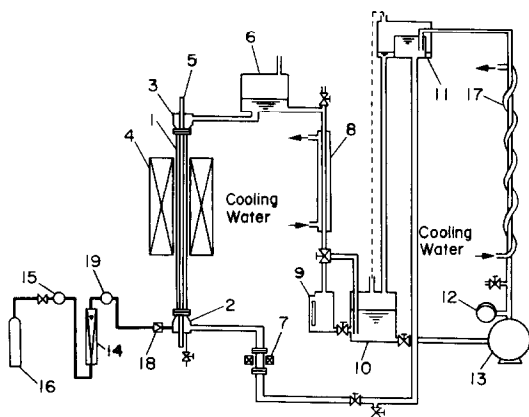


FIG. 1. Experimental apparatus: (1) test section; (2) lower mixing chamber; (3) upper mixing chamber; (4) magnet; (5) heater; (6) separator; (7) electromagnetic flowmeter; (8) cooler; (9) flow rate measuring tank; (10) lower tank; (11) upper tank; (12) accumulator; (13) pump; (14) rotameter; (15) constant pressure regulator; (16) argon gas; (17) cooler; (18) check valve; (19) pressure gauge.

EXPERIMENTAL APPARATUS AND PROCEDURES

Experiments were carried out using the mercury loop of the Nuclear Power Experiment Facility in the Department of Nuclear Engineering, Kyoto University.

The experimental arrangement is shown schematically in Fig. 1. Distilled mercury is forced up by the diaphragm pump 13 from the lower tank 10 to the upper tank 11 where the liquid level is kept constant. All free surfaces of liquid mercury are covered by argon gas to prevent the oxidization of mercury. From the upper tank the mercury flows downwards and enters the mixing chamber 2, where the argon gas is injected through three 6 mm dia stainless steel tubes merging into the mercury. As shown in Fig. 2, each tube has 20 holes of 0.8 mm dia. The mercury–argon two-phase mixture flows upwards in a vertical circular lucite tube 1 of $D_o = 19$ mm I.D., in which the 304 stainless steel sheathed electrical heater of $D_i = 6$ mm O.D. is concentrically installed by using three spacers as shown in Fig. 3. Subsequently, the argon gas is separated in the phase-separator 6, and only the mercury returns to the lower tank 10. The upper tank and the separator are 4 and 3 m above the ground respectively, and therefore there is a head difference of 1 m to circulate the mercury. The flow rates of both fluids are measured by the electromagnetic flowmeter 7 and rotameter 14, respectively.

The test section 1 is placed at the 30 mm wide gap between the magnetic pole pieces which are 50 mm wide and 1000 mm long as shown in Fig. 3. The distribution of the magnetic flux is uniform, and its maximum density is 0.7 T. The upstream extremity of the magnetic field coincides with that of the heating section, and this position is defined as $x = 0$. The equivalent diameter of this annulus is $d_c = 13$ mm. The inconel sheathed alumel–chromel thermocouples of

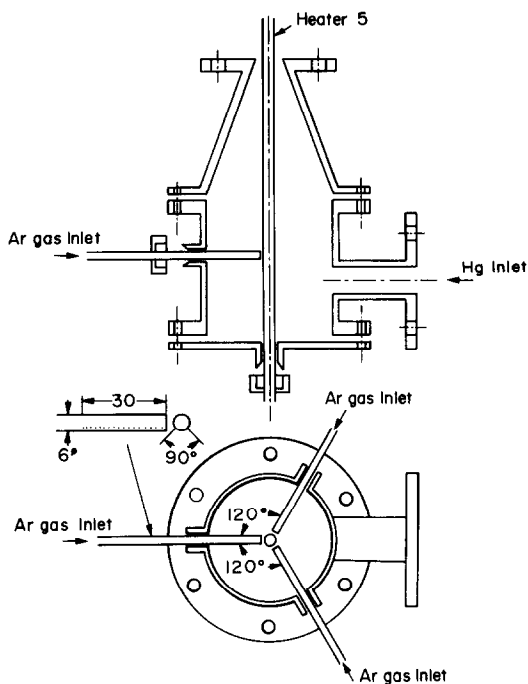


FIG. 2. Mixing chamber.

0.3 mm O.D. are welded on the heater surface at the positions L_1 – L_5 corresponding to x/d_c shown in Fig. 3. The L_6 thermocouple is welded just opposite side of L_5 . The fluid temperatures at the inlet and the outlet are measured by 316 stainless steel sheathed alumel–chromel thermocouples in the mixing chambers 2 and 3 respectively.

The local properties of two-phase flow at the positions L_4 and L_5 are measured by using the same double-sensor probe (electrical resistivity probe) together with the same electronic equipment as those developed for the investigation of water–air two-phase flow, which have been reported by Serizawa *et al.* [10]. In order to measure radial distributions of local void fraction, bubble number rate and bubble velocity, the double-sensor probe is radially traversed in sides A and B as shown in Fig. 4. Side B is just opposite A.

The ranges of flow variables covered in this experimental study are: mercury flow rate $W_L = 0.42$ – 1.25 kg s^{-1} , its Reynolds number $Re = 1.36 \times 10^4$ – 4.1×10^4 , its Peclet number $Pe = 372$ – 1100 , its Hartmann number $M = 0$ – 110 , argon gas flow rate $W_G = 2.63 \times 10^{-6}$ – 8.49×10^{-6} kg s^{-1} , quality $x_q = 2.87 \times 10^{-4}$ – 1.72×10^{-3} %, inlet fluid temperature 11.5– 18.8°C , and heat flux $q = 1.33 \times 10^4$ – 2.21×10^4 W m^{-2} .

The physical properties of mercury were taken from Schmücker [11].

EXPERIMENTAL RESULTS AND DISCUSSION

First of all, when no magnetic field is present, it is very important to confirm the heat transfer coefficient

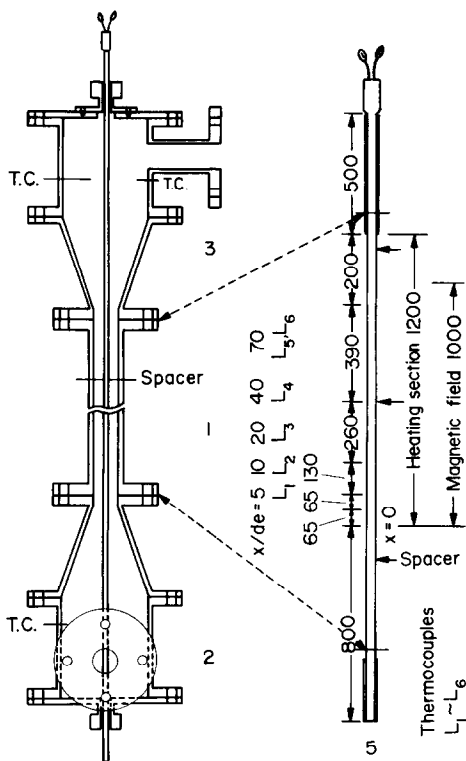


FIG. 3. Test section.

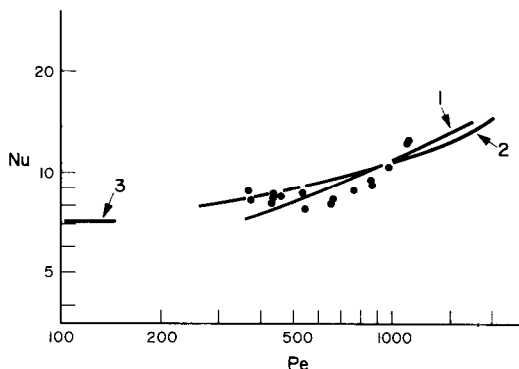


FIG. 5. Developed heat transfer of single phase mercury flow : $B = 0$; $x/d_e = 70$. Curve 1, $Nu = 6.8023 + 0.0214(\Psi Pe)^{0.7956}$, $\Psi = 1 - 1.82/Pr(\epsilon_M/v)_{max}^{1.4}$, $(\epsilon_M/v)_{max} = 4.0 + 0.002897 Re^{0.919}$; Curve 2, $Nu = 6.886 + 5.578 \times 10^{-3} (Pe)^{0.9427}$; Curve 3, $Nu = 7.11$.

of single phase mercury flow in the annulus of which radius ratio R_i/R_o is 0.315. Figure 5 shows the experimental data of Nusselt number Nu in the developed region ($x/d_e = 70$), where $Nu = qd_e / [(T_w - T_{bk})\lambda_L]$, and T_w , T_{bk} and λ_L are the heater surface temperature at x , bulk temperature of fluid at x which is calculated by the linear interpolation between the inlet and the outlet fluid temperatures, and thermal conductivity of mercury, respectively. In this figure, curve 1 shows the theoretical results of Dwyer and Tu [12] and curve 2 the results of Michiyoshi and Nakajima [13], for developed turbulent heat transfer of liquid metal in the case of uniform heat flux at the inner wall and thermally insulated at the outer wall of the annulus of 0.315 radius ratio. Agreement between experiments and theories is satisfactory. Curve 3 shows the theoretical results of Michiyoshi [14] for developed laminar heat transfer in case of the same conditions as mentioned above. For the turbulent heat transfer in the thermal entrance region, comparison of experiments with the theory of Michiyoshi and Nakajima [15] is illustrated in Fig. 6. This figure also shows satisfactory agreement. These results imply that there is no fouling effect on heat transfer in the present experiments.

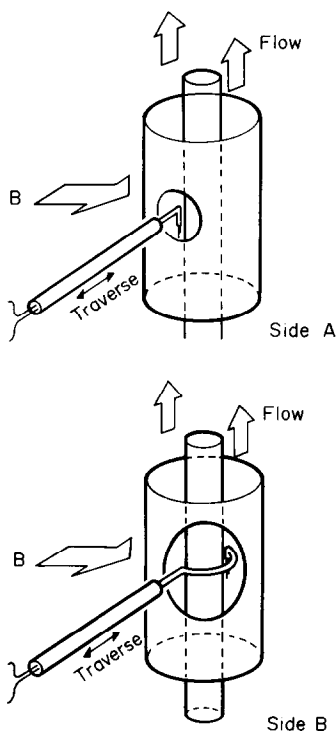


FIG. 4. Double-sensor probes.

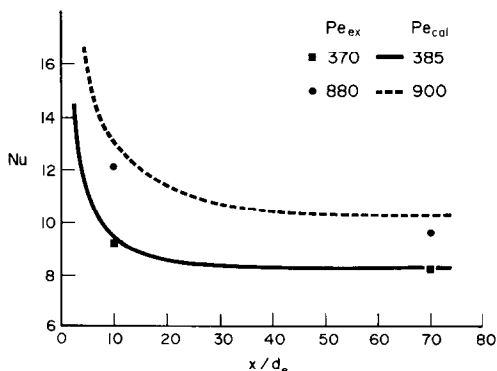


FIG. 6. Turbulent heat transfer in thermal entrance region of single phase mercury flow, $B = 0$.

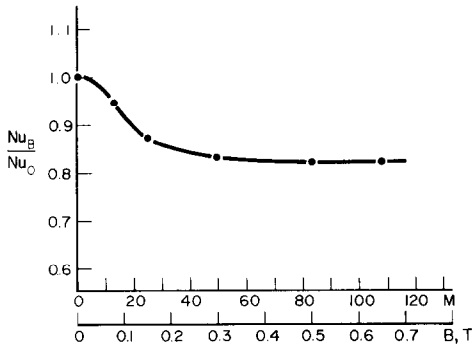


FIG. 7. Effect of magnetic field on single phase mercury heat transfer, $x/d_e = 70$, $Pe = 440$, $Nu_0 = 8.25$.

One example of the effect of magnetic field on the heat transfer of single phase mercury flow at $x/d_e = 70$ is shown in Fig. 7, where Nu_B and Nu_0 are Nusselt numbers, which are already defined, for $B \neq 0$ and $B = 0$ respectively. It can be seen that Nu_B decreases with Hartmann number M and it becomes about 80% of Nu_0 at the fixed Peclet number Pe . When M is fixed, Nu_B decreases once, but it recovers from the minimum value with increasing Pe for small M as shown in Fig. 8. This is caused by turbulent-laminar-turbulent flow transition. Similar tendencies have been already pointed out by Gardner *et al.* [16] (broken line) and Michiyoshi *et al.* [17] (chain line) for a circular tube, and Kitamura *et al.* [18] for a rectangular channel. In [17], since the cover gas was not used the fouling affected the heat transfer coefficients. Therefore, the thermal resistance due to fouling obtained from the data of heat transfer for $B = 0$ was applied directly to the heat transfer for $B \neq 0$. Thus the chain line in Fig. 8 might involve an error due to such correction. However, there is no effect of fouling in the present experiments as mentioned above.

Now we discuss the local properties of mercury-argon two-phase flow in the vertical annulus of 0.315 radius ratio. One example of radial distributions of bubble number rate N_{loc} count min^{-1} and local void fraction α_{loc} % measured at the position $x/d_e = 40$ by eliminating the spacer at this position (Fig. 3) and also

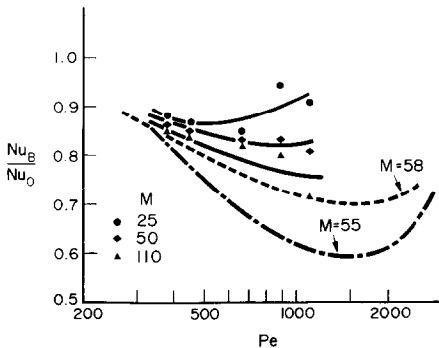


FIG. 8. Effect of Peclet number on single phase mercury heat transfer under magnetic field; $x/d_e = 70$.

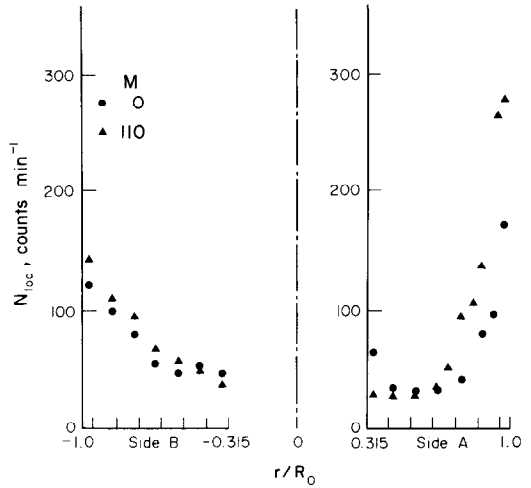


FIG. 9. Radial distribution of bubble number rate, N_{loc} . $x_q = 1.49 \times 10^{-3}\%$; $Pe = 440$; $x/d_e = 40$.

bubble velocity V_b $m s^{-1}$ at $x/d_e = 70$ is shown in Figs. 9, 10 and 11, respectively. Large gas slugs were not observed through the transparent lucite tube so far as we observed gas bubbles flowing along the outer wall of the annulus. This fact appears in Fig. 10. The α_{loc} profile is similar to that of water-air bubbly flow in a vertical annulus [7], and it is not convex-shaped shown in the previous paper [9] for slug flow but saddle-shaped. Especially, the α_{loc} is smaller near the inner wall (heater surface) and it is large near the outer wall of the annulus. From these facts, the two-phase flow pattern might be bubbly flow. Effects of magnetic field on the α_{loc} and N_{loc} are not significant in this experiment, but a little decrease in them can be seen near the inner wall. This tendency is the same as that reported in the previous paper [9]. The radial profile of α_{loc} in the direction perpendicular to the magnetic field (Fig. 4) is almost symmetric with respect to the channel axis. Although the radial profile of α_{loc} in the direction

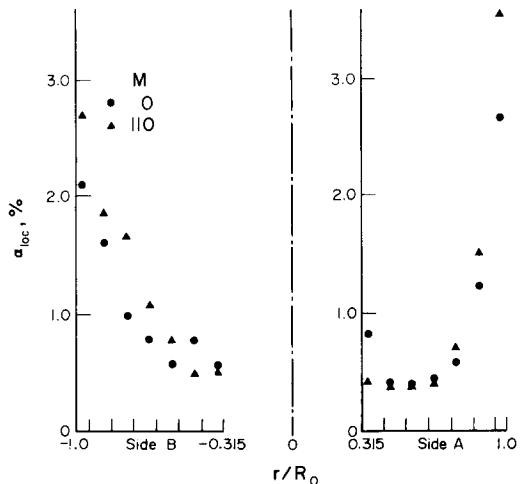


FIG. 10. Radial distribution of local void fraction, α_{loc} . $x_q = 1.49 \times 10^{-3}\%$; $Pe = 440$; $x/d_e = 40$.

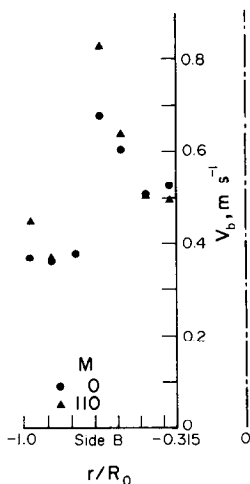


FIG. 11. Radial distribution of bubble velocity, V_b , $x_q = 7.15 \times 10^{-4}\%$. $Pe = 440$; $x/d_e = 70$; $u_m = 14 \text{ cm s}^{-1}$.

parallel to the magnetic field was not measured it might be almost identical with that in the direction perpendicular to the magnetic field according to the previous paper [9].

The bubble velocity V_b is much larger than the superficial velocity of mercury u_m (Fig. 11). Such characteristics result from the large density ratio of mercury to argon gas as derived from the equation of slip ratio,

$$\frac{V_G}{V_L} = \frac{x_q}{1-x_q} \frac{1-\alpha}{\alpha} \frac{\rho_L}{\rho_G}$$

and it will cause the agitation of bubbles, and hence an increase in the eddy diffusivity of heat ε_{HTP} of two-phase flow [7, 8, 10]. It can be also seen that the magnetic field causes a little increase of V_b , especially at $|r/R_0| > 0.6-0.7$. These results show the same tendency as that in the ref. [9] but the eddy diffusivity ε_{HTP} does not seem to be increased further under the magnetic field in the present experiments. Mori *et al.* [19] have studied experimentally the effect of magnetic field on the motion of a single nitrogen bubble rising through still mercury, but their data can not be applied directly to the two-phase flow which contains many bubbles in flowing mercury. Dunn [20] discussed the effect of M-

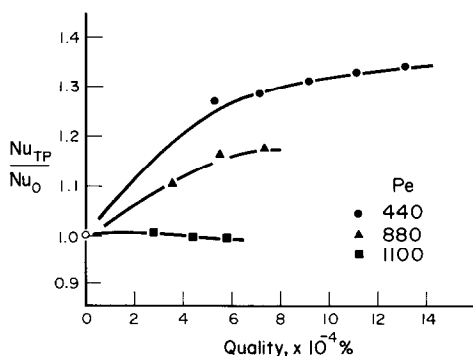


FIG. 12. Two-phase heat transfer; $B = 0$; $x/d_e = 70$.

shaped velocity profile on the two-phase pressure differences. While the local velocity of liquid (mercury) also increases in this present two-phase flow, its large increase will not be expected since the local void fraction is small (Fig. 10).

When no magnetic field is present, the two-phase heat transfer data obtained at $x/d_e = 70$ in this experiment are shown in Fig. 12, where Nu_{TP} and Nu_0 are Nusselt numbers for two-phase flow and single phase mercury flow respectively, and their definition is the same as aforementioned. When Peclet number Pe is small, Nu_{TP} becomes larger than Nu_0 with increasing quality x_q . This tendency is similar to that obtained for the water-air two-phase flow in vertical annulus [7]. When Pe is large ($Pe = 1100$), however, Nu_{TP}/Nu_0 is nearly equal to unity and Nu_{TP} becomes smaller than Nu_0 . Since the local void fraction α_{loc} is small near the heater surface as already pointed out in Fig. 10, the effective thermal conductivity of two-phase flow scarcely decreases if we adopt the Maxwell equation

$$\lambda_{\text{TP}} = \lambda_L \frac{1 - \alpha_{\text{loc}}}{1 + 0.5\alpha_{\text{loc}}}$$

Thus the enhancement of Nu_{TP} might be contributed mainly by the increase of ε_{HTP} as already mentioned. On the other hand, when Pe is large ($Pe = 1100$), since the eddy diffusivity of heat of mercury flow is large in itself, it might be said that the agitation of bubbles scarcely contributes to the heat transfer enhancement. Mizushina *et al.* [2] and Ochiai *et al.* [3] made use of circular tube, and they did not measure radial distributions of local void fraction, bubble velocity and so on. Since bubbles are apt to gather near the tube wall (heating surface), the decrease of heat transfer coefficient in their experiments might be eminently due to the decrease of effective thermal conductivity. In this connection, Winterton's theory [5] has shown that a layer of gas bubbles covering the wall surface (heating surface) of circular tube, in which the liquid metal flows with uniform velocity profile, lowers the heat transfer, by considering only the heat conduction. Recently Bishop *et al.*'s [6] analysis also shows the reduction in heat transfer of sodium-gas two-phase flow with similar considerations. It should be noted, however, that the two-phase heat transfer is affected by various local properties of two-phase flow as mentioned above.

Except for $Pe = 1100$, Fig. 13 illustrates the correlation of Nu_{TP}/Nu_0 against Lockhart-Martinelli modulus χ_{li} ,

$$\chi_{\text{li}} = \left(\frac{1-x_q}{x_q} \right)^{0.9} \left(\frac{\rho_G}{\rho_L} \right)^{0.5} \left(\frac{\mu_L}{\mu_G} \right)^{0.1}$$

and

$$Nu_{\text{TP}} = Nu_0 [1 + 118 \chi_{\text{li}}^{-0.911}] \quad (1)$$

This correlation obtained at $x/d_e = 70$ covers the range of Peclet number of 400-900, or $Nu_{\text{TP}}/Nu_0 > 1$. It is similar to the water-air two-phase heat transfer [7].

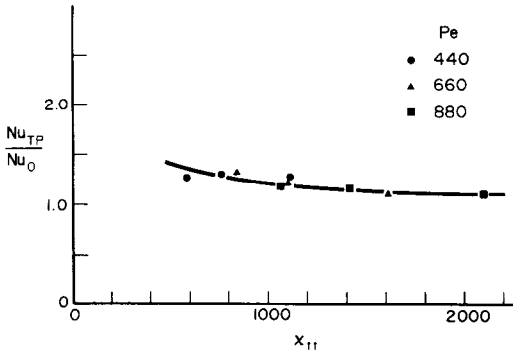


FIG. 13. Correlation of two-phase heat transfer against Lockhart-Martinelli modulus, $400 < Pe < 900$, $x/d_e = 70$, $B = 0$.

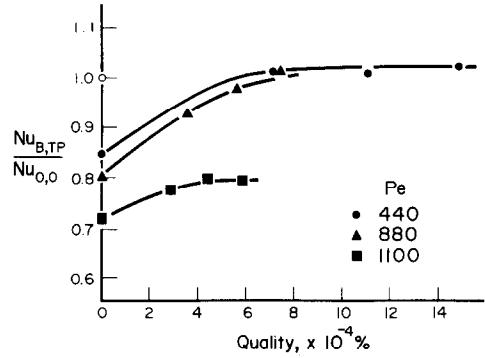


FIG. 15. Effect of quality on two-phase heat transfer under magnetic field, $M = 110$, $x/d_e = 70$.

Last of all, we discuss the effect of magnetic field on the two-phase heat transfer. In Figs. 14 and 15, $Nu_{B,TP}$ and $Nu_{0,0}$ are Nusselt numbers for two-phase flow in $B \neq 0$ and for single phase mercury flow in $B = 0$, respectively. Thus $Nu_{0,0}$ is identical with Nu_0 shown in Figs. 12 and 13. With increasing Hartmann number M at the fixed Peclet number Pe , the two-phase Nusselt number decreases as well as single phase mercury heat transfer, but its decrease becomes smaller than the single phase as x_q is increased. This is clearly shown by the following correlation obtained from Fig. 14:

For single-phase mercury flow;

$$Nu_B = Nu_0 \exp\left(-0.23 \frac{M}{80}\right), M < 83 \quad (2)$$

For two-phase flow; $Nu_{B,TP} = Nu_{TP} \exp\left(-0.23 \frac{M}{120}\right)$, $1075 < \chi_{11} < 2100$, $M < 83$. (3)

In this correlation, Nu_{TP} is the two-phase Nusselt number for $B = 0$ and the same as that in equation (1). Thus we can derive $Nu_{B,TP}/Nu_0$ from equations (3) and (1), where $Nu_0 = Nu_{0,0}$. These correlation curves are shown in Fig. 14.

These facts indicate that since further increase of ϵ_{HTP} due to the agitation of bubbles is not expected under the magnetic field in the present experiment as

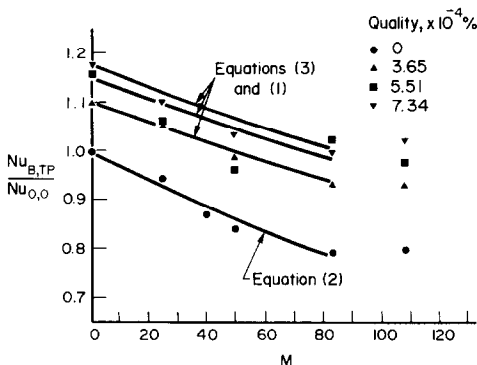


FIG. 14. Effect of magnetic field on two-phase heat transfer, $x/d_e = 70$, $Pe = 880$, $Nu_{0,0} = 9.34$.

mentioned, the suppression of mercury flow velocity caused by the Lorentz force mainly contributes to the reduction of heat transfer even in the two-phase flow, and it is weakened in the two-phase flow because the void fraction lowers the effective electrical conductivity.

The relationship between $Nu_{B,TP}/Nu_{0,0}$ and quality x_q at the fixed M is shown in Fig. 15. From Figs. 15 and 14, it can be seen that the heat transfer of single phase mercury flow decreases because of the effect of magnetic field, but the heat transfer under magnetic field recovers to that under non-magnetic field by introducing some small quantity of gas into the liquid when Pe is small. However, this is not the case when Pe is large.

CONCLUSIONS

Experimental data of local properties and heat transfer of mercury-argon two-phase bubbly flow with small gas flow rate in vertical annulus in the presence of transverse magnetic field have shown that the two-phase Nusselt number decreases as well as single phase mercury heat transfer with increasing Hartmann number at the fixed Peclet number, but its decrease becomes smaller than the single phase as the quality is increased. Empirical correlations (1)-(3) clearly show these characteristics. Taking into consideration the local void fraction, bubble velocity and so on, we have discussed the effective thermal conductivity, eddy diffusivity of heat and liquid velocity to clarify their contributions to the heat transfer of two-phase flow with and without magnetic field. Future study should be conducted to widen the range of flow variables. In this connection, alkali metal-gas two-phase heat transfer is an interesting subject since the alkali metal holds high thermal and electrical conductivities and low density as compared with mercury.

REFERENCES

1. O. Lielausis, Liquid-metal magnetohydrodynamics, *Atom. Energy Rev.* **13**, 527-581 (1975).
2. T. Mizushima, T. Sasano, M. Hirayama, N. Otsuki and M. Takeuchi, Effect of gas entrainment on liquid metal heat transfer, *Int. J. Heat Mass Transfer* **7**, 1419-1425 (1964).

3. M. Ochiai, T. Kuroyanagi, K. Kobayashi and K. Furukawa, Void fraction and heat transfer coefficient of sodium-argon two-phase flow in vertical channel, *J. Atom. Energy Soc. Japan* **13**, 566-573 (1971).
4. M. Hori and A. J. Friedland, Effect of gas entrainment on thermal-hydraulic performance of sodium cooled reactor core, *J. Nucl. Sci. Technol.* **7**, 256-263 (1970).
5. R. H. S. Winterton, Effect of gas bubbles on liquid metal heat transfer, *Int. J. Heat Mass Transfer* **17**, 549-554 (1974).
6. A. A. Bishop, F. C. Engel and R. A. Markley, Heat transfer effect of entrained gas in liquid sodium systems, *Nucl. Engng Des.* **52**, 1-13 (1979).
7. I. Michiyoshi, Heat transfer in air-water two-phase flow in a concentric annulus, Heat Transfer, Toronto (6th Int. Heat Transfer Conf.), Vol. 1, pp. 499-504 (1978).
8. I. Michiyoshi, Two-phase two-component heat transfer, Heat Transfer, Toronto (6th Int. Heat Transfer Conf.), Vol. 6, pp. 219-233 (1978).
9. I. Michiyoshi, H. Funakawa, C. Kuramoto, Y. Akita and O. Takahashi, Local properties of vertical mercury-argon two-phase flow in a circular tube under transverse magnetic field, *Int. J. Multiphase Flow* **3**, 445-457 (1977).
10. A. Serizawa, I. Kataoka and I. Michiyoshi, Turbulence structure of air-water bubbly flow, *Int. J. Multiphase Flow* **2**, 221-233; **2**, 235-246; **2**, 247-259 (1975).
11. H. Schmücker, Sieden von Quecksilber im senkrechten Rohr bei Zwangskonvektion und niedrigen Drücken, Technische Universität München, Dr.-Ing. dissertation (1974).
12. O. E. Dwyer and P. S. Tu, Unilateral heat transfer to liquid metals flowing in annuli, *Nucl. Sci. Engng* **15**, 58-68 (1963).
13. I. Michiyoshi and T. Nakajima, Heat transfer in turbulent flow with internal heat generation in concentric annulus, (I) Fully developed thermal situation, *J. Nucl. Sci. Technol.* **5**, 476-484 (1968).
14. I. Michiyoshi, Heat transfer in laminar flow with internal heat generation in concentric annulus, *J. Nucl. Sci. Technol.* **3**, 479-485 (1966).
15. I. Michiyoshi and T. Nakajima, Heat transfer in turbulent flow with internal heat generation in concentric annulus, (II) Thermal entrance region, *J. Nucl. Sci. Technol.* **7**, 26-33 (1970).
16. R. A. Gardner, K. L. Uherka and P. S. Lykoudis, Influence of a transverse magnetic field on forced convection liquid metal heat transfer, *AIAA JI* **4**, 848-852 (1966).
17. I. Michiyoshi, K. Takitani and T. Amano, Liquid mercury heat transfer in circular tube under transverse magnetic field, *J. Atom. Energy Soc. Japan* **10**, 183-189 (1968).
18. K. Kitamura, A. Yasukawa and M. Hirata, Experimental investigation of a liquid metal flow and heat transfer under a transverse magnetic field, 2nd Report, Heat transfer for a rectangular channel flow, *Trans. Japan Soc. Mech. Engrs* **46B**, 962-970 (1980).
19. Y. Mori, K. Hijikata and I. Kuriyama, Experimental study of bubble motion in mercury with and without a magnetic field, *Trans. Am. Soc. Mech. Engrs, Series C, J. Heat Transfer* **99**, 404-410 (1977).
20. P. F. Dunn, Single-phase and two-phase magnetohydrodynamic pipe flow, *Int. J. Heat Mass Transfer* **23**, 373-385 (1980).

TRANSFERT THERMIQUE D'UN FLUIDE DIPHASIQUE MERCURE-ARGON DANS UN ESPACE ANNULAIRE VERTICAL AVEC CHAMP MAGNETIQUE TRANSVERSE

Résumé—On présente des expériences sur les propriétés locales et sur le transfert thermique d'un écoulement diphasique mercure-argon avec un faible débit de gaz, dans un espace annulaire vertical en présence d'un champ magnétique transverse. Le nombre de Nusselt décroît comme dans le cas de la phase unique de mercure, lorsque le nombre de Hartmann augmente à nombre de Peclet fixé, mais sa décroissance est de plus en plus faible quand la qualité augmente. On discute les contributions sur le transfert de chaleur des conductivités thermiques, de la diffusivité thermique turbulent et de vitesse du liquide.

ZWEIPHASEN-WÄRMEÜBERTRAGUNG ZWISCHEN QUECKSILBER UND ARGON IN EINEM VERTIKALEN RINGSPALT—UNTER DEM EINFLUSS EINES QUER ZUR STRÖMUNGSRICHTUNG VERLAUFENDEN MAGNETFELDES

Zusammenfassung—In dieser Arbeit werden experimentelle Ergebnisse über örtliche Stoffeigenschaften und den Wärmetransport in einer Quecksilber/Argon-Zweiphasen-Blasenströmung mit kleinem Gasströmungsanteil in einem vertikalen Ringspalt unter dem Einfluß eines quer zur Strömungsrichtung orientierten Magnetfeldes mitgeteilt. Sowohl die Nusselt-Zahl der Zweiphasenströmung als auch der Einphasen-Wärmeübergang des Quecksilbers nimmt mit zunehmender Hartmann-Zahl für eine bestimmte Peclet-Zahl ab, aber diese Abnahme ist geringer als die der flüssigen Phase bei Vergrößerung des Dampfgehaltes. Der Beitrag der effektiven thermischen Leitfähigkeit und des turbulenten Wärme- und Impulstransportes zum Zweiphasen-Wärmeübergang werden erörtert.

ТЕПЛОПЕРЕНОС ПРИ ДВУХФАЗНОМ ТЕЧЕНИИ СМЕСИ РТУТЬ-АРГОН В ВЕРТИКАЛЬНОЙ КОЛЬЦЕВОЙ ТРУБЕ С ПОПЕРЕЧНО ПРИЛОЖЕННЫМ МАГНИТНЫМ ПОЛЕМ

Аннотация—Представлены экспериментальные данные по локальным характеристикам и теплообмену при двухфазном пузырьковом течении смеси ртуть-аргон по вертикальной кольцевой трубе в поперечном магнитном поле при малых скоростях течения газа. Показано, что с увеличением числа Хартмана при фиксированном числе Пекле значение числа Нуссельта для двухфазного потока, как и для однофазного течения ртути, снижается, однако при увеличении содержания газа это снижение становится меньшим, чем для однофазного потока. Рассматривается влияние на двухфазный теплообмен эффективной теплопроводности, вихревой диффузии тепла и скорости жидкости.